# Improvements in Power Quality and Efficiency with a new AC/DC High Current Converter

FRANCESCO MUZI, LUIGI PASSACANTANDO
Department of Electrical Engineering and Computer Science
University of L'Aquila
Piazzale Pontieri, 1 - L'Aquila 67100
ITALY
muzi@ing.univaq.it luigi.passacantando@tiscali.it

*Abstract:* - A very flexible AC/DC converter featuring high-output current, reduced voltage ripple and highly adjustable current control is described. The whole system consists of four stages and uses a proper switching technique in conjunction with a feedback control performed by means of a PID regulator. Moreover, the built prototype exhibits high efficiency and reduced harmonic pollution. In order to evaluate the harmonic distortion on the current drawn from the supply network, an FFT (Fast Fourier Transform) analysis is performed. Finally, experimental and computation results for output currents up to 400A, which confirm the correct behavior of the proposed converter, are presented and discussed.

*Key-Words:* - AC/DC converter, High direct-current, FFT, Electrical distribution systems, Power quality.

## 1 Introduction

In the last few decades, a continuous integration process between electrical systems and power electronic apparatuses has been observed. Power electronics, which has been applied so far mainly to energy end uses [1], was recently employed also in distributed generation, namely photovoltaic and wind generation. Actually, the ever-growing exploitation of renewable sources requires that voltage and current wave shapes should be compatible with current power distribution. On the other hand, new architectures for modern electrical systems have been developed, and novel active filtering techniques and devices have been proposed, which will be able to change the power factor and to eliminate undesired harmonics as well [3], [4], [5], [6], [7]. In order to modify the power factor, either deterministic digital techniques or probabilistic approaches were usually adopted [8], [9]. In addition, AC/DC converters were actively researched in order to improve the power factor at reasonable costs. From this point of view, both the use of a PCB (Printed Circuit Board) and implementation of a proper switching control technique allowed a drastic reduction of manufacturing costs. As a matter of fact, the adoption of these techniques achieved over 90% cost reduction [10]. Unfortunately, the controlled switching produced electromagnetic emissions (EMI) causing disturbances to radio frequencies (RF). A number of studies pointed to a control procedure of power supply switching with modulation techniques of the RPWM type (*Random Pulse Width Modulation*) that performed much better than PWM (*Pulse Width Modulation*) [11]. Other studies aimed at reducing non-characteristic harmonics [12]. Also resonant filters were proposed for high power AC/DC converters adopting tyristors, where a parallel resonance was used to obtain amplification of selected harmonics applying a sort of filtering technique [13]. Optimization studies were also performed on AC/DC converters with synchronous rectification, that can be used to supply electrical machines requiring high direct currents, with an aim to reduce losses at the output stage of the converter. In this case a MOSFET, which performs a role similar to a switching power supply, and a resistive load are parallel-connected at the output of the generator. An AC/DC converter built with a synchronous machine and a parallel-connected power MOSFET allow a reduction of the losses on the DC output supply stage [15].

In this paper a high current AC/DC converter with high quality performance is introduced. The whole system is described and experimental results obtained from experimental tests performed on a built prototype are reported, analyzed and discussed.

## 2 The proposed system

The proposed converter is schematically shown in Fig. 1.

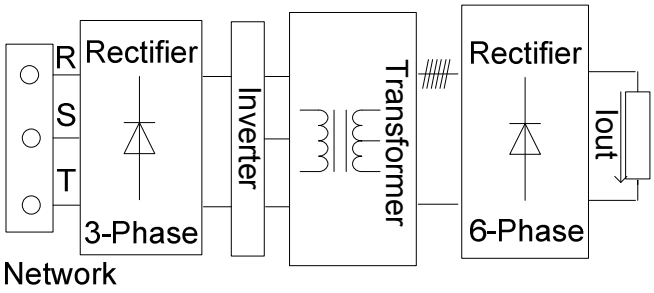


Fig. 1 Layout of the proposed four-stage system.

The first stage of the system consists of a 6-diode passive rectifier. The rectified voltage is applied to an inverter that in its turn is made of an ultra-fast 6-IGBT able to commute up to 100 kHz under certain operating conditions. The value of the rectified voltage was about 500 V, neglecting a ripple that can be reduced placing an active rectifier at the input terminations of the inverter. Two serially-connected capacitors, each of 2200 μF, were placed between the DC bus and frame to achieve additional voltage smoothening. The modulation technique adopted to drive the inverter was strongly characterized by the 6-phase transformer/rectifier system used.
The scheme of the three-phase inverter is shown in Fig. 2 where the phase-neutral, phase-to-phase voltages and command signals of the three legs of the inverter are also reported.

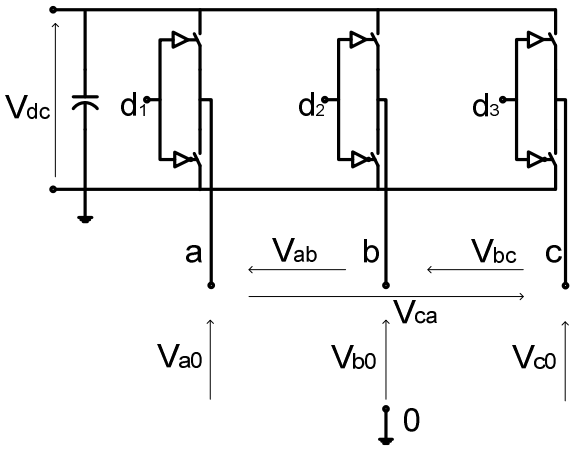


Fig. 2 Scheme of a three-phase inverter.

The modulation technique adopted to drive the three legs of the inverter is shown in Fig 3. This technique was implemented taking in mind the configuration of the downstream transformer.

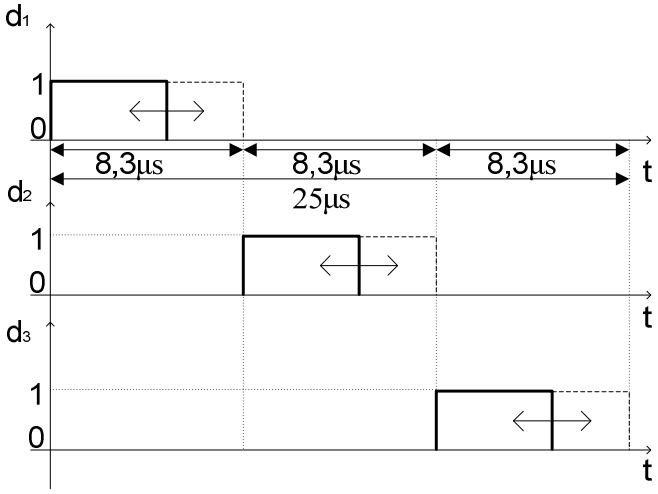


Fig. 3 Signals used to drive the inverter.

Fig. 3 shows that the voltage time period for each phase is 25 μs. Each phase terminal (phases a, b, c) is connected by the respective IGBTs for a maximum time of 8,3 μs (depending on the command processed by the modulation) to a "+Vdc" potential while for the remaining 16,6 μs of the time period the same terminal is connected to ground. In other words, each phase-neutral voltage ($V_{a0}$, $V_{b0}$ *e* $V_{c0}$) is a rectangular wave having *+Vdc* amplitude and period of 25 μs. The duty cycle of this rectangular wave can change between a maximum of 33% (8,3 μs) and a minimum of 0% (0 μs). Fig. 4 shows the three phase-neutral voltages.

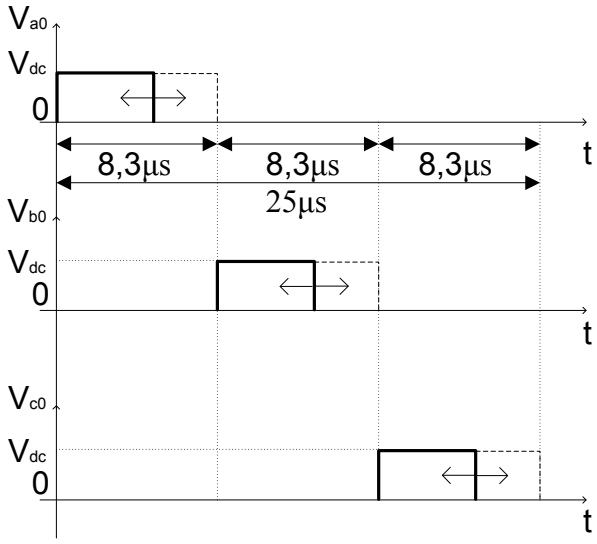


Fig. 4 Phase-neutral voltages of the inverter.

The phase-to-phase voltages are linked to the phase-neutral voltages by the following well-known relations:

$$V_{ab} = V_{a0} - V_{b0} \quad (1)$$
$$V_{bc} = V_{b0} - V_{c0} \quad (2)$$
$$V_{ca} = V_{c0} - V_{a0} \quad (3)$$

It is also known that the phase-to-phase voltages ($V_{ab}$, $V_{bc}$,$V_{ca}$) can assume both positive and negative values, whereas phase-neutral voltages ($V_{a0}$, $V_{b0}$ *e* $V_{c0}$) take up only positive values. Fig. 5 shows the shapes of the ($V_{ab}$, $V_{bc}$, $V_{ca}$) phase-to-phase voltages.

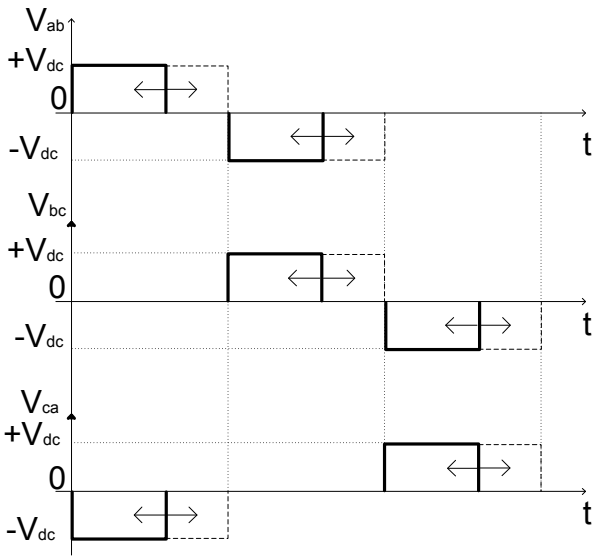


Fig. 5 Wave shapes of phase-to-phase voltages.

The phase-to-phase voltage generated downstream of the inverter is applied at the input terminations of the 6-phase transformer/rectifier block shown in Fig. 6.

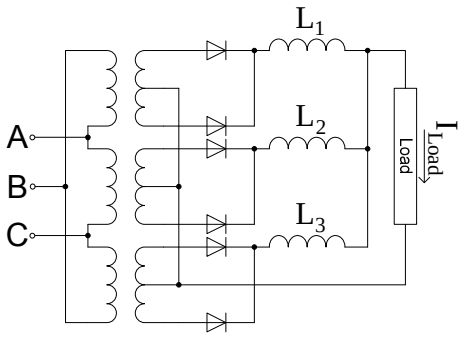


Fig. 6 Six-phase transformer/rectifier block supplying the load.

The transformer reduces the voltage while increasing the current. The working principle of the sub-system shown in Fig. 6 is illustrated in Fig. 7.

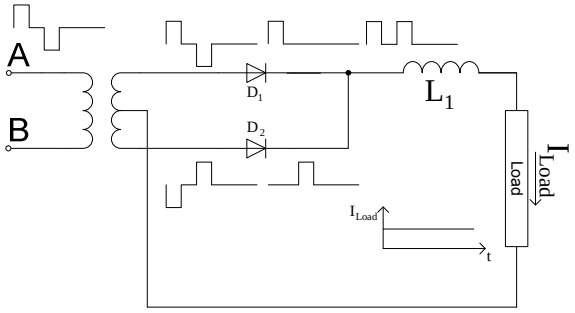


Fig. 7 Working scheme of the transformer and AC/DC rectifier.

Of course, the $L_1$, $L_2$ and $L_3$ inductors shown in Figs. 6 and 7 were used to smoothen the load current. The whole system shown in Fig. 1 is driven by a DSP (Digital Signal Processor), model *dsPIC30F3011* of the Microchip family [16].

## 2.3 Control scheme of the converter

In order to obtain the desired output current values, the scheme of Fig. 1 was completed by a proper feedback control system as shown in Fig. 8.

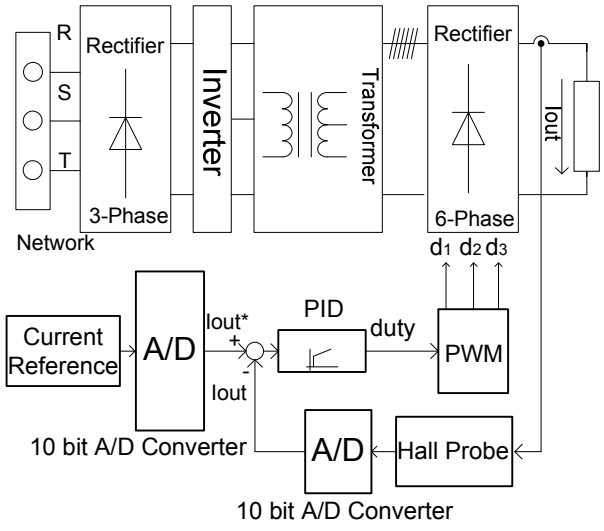


Fig. 8 Block diagram of the output-current control system.

The adopted control technique was implemented by means of a PID regulator. A block diagram of the adopted feedback control is shown in Fig. 9.
As already said in section 2, the whole control system was implemented on a proper, DSP-managed card.

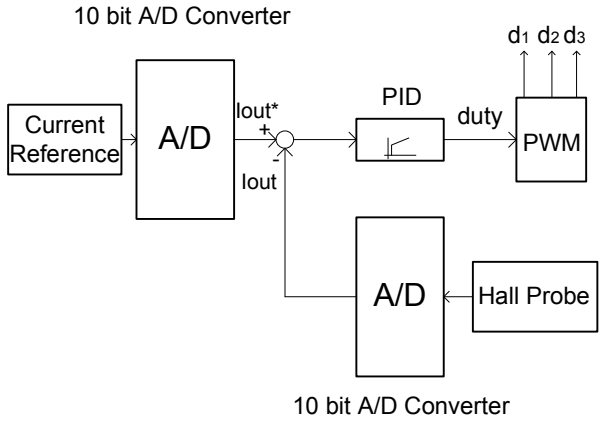


Fig. 9 Block diagram of the feedback control of the current.

The output current value was monitored using a control strategy consisting of a PID regulator with a soft-start technique. Since the output load is connected to smoothing inductances, in order to avoid sudden changes of the output current, the program emulating the PID regulator was completed with a proper section able to manage current changes smoothly. As a matter of fact, the control actions fine-tuned the rise and fall fronts of the output current in order to protect the smoothing inductances connected downstream the transformer against negative consequences. In addition, Fig. 9 shows that the input quantities of the feedback section are the output current values obtained from a measurement system placed proximally to the load, and of course also the current external pre-established reference value. Measured currents and reference current are analogical in nature. Consequently, these current signals must be transformed into digital data to be sent to the DSP, which justifies the use of 10-bit converters placed inside the DSP. The output signals produced by the feedback section are $d_1$, $d_2$ and $d_3$, which in their turn drive the three legs of the inverter in accordance to the previously explained technique.

## 3 Harmonic analysis of the current drawn from the supply network

The ever-growing complexity of electrical systems requires the development of apparatuses able to monitor and regulate working conditions continuously. For this reason, computation algorithms were implemented that, on the basis of measurements at certain system points were able to establish the real-time working system state [16], [17], [18], [23], [24]. The data supplied from the measurements and acquired on electrical apparatuses can be properly processed by means of a number of algorithms such as the FFT algorithm, which is commonly used to improve the quality of samples obtained from the measurement system [19], [25].

In this paper, the FFT is used to monitor the harmonic content of the wave shape of the current drawn from the supply network. The algorithm processes current samples acquired by means of a measurement system placed between the network and the input terminations of the three-phase rectifier as shown in Fig. 10.

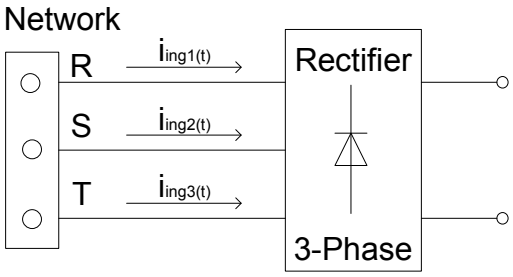


Fig. 10 Currents acquired by the measurement system for the subsequent FFT analysis.

For simplicity reasons, in the following the performed harmonic analysis is illustrated only for the R-phase current, since the shapes of all currents of the three-phase system are equal and shifted 120° from one another.

Assuming the series $i_{in}(n)=i_{in}(n\Delta t)$ obtained from the $N$ coming samples of the measured $i_{in}(t)$ current, the DFT (Discrete Fourier Transform) can be expressed as:

$$I_{in}(k\Delta f)=\Delta t\sum_{n=0}^{N-1} i_{in}(n\Delta t)\cdot e^{-j2\pi k\Delta f n\Delta t} \quad (4)$$

where $\Delta f$ is the frequency sample interval (computed using the following relation: $\Delta f=1/N\Delta t$) and $\Delta t$ is the sampling time. The inverse discrete Fourier transform is:

$$i_{in}(n\Delta t)=\Delta f\sum_{k=0}^{N-1} I_{in}(k\Delta f)\cdot e^{j2\pi k\Delta f n\Delta t}\ . \quad (5)$$

In order to simplify relation (4), the quantities $\Delta t$ and $\Delta f$ can be omitted obtaining the following notation:

$$I_{in}(k)=\sum_{n=0}^{N-1} i_{in}(n)\cdot e^{-j2\pi kn/N} \quad (6)$$

In the same way, relation (5) can be written as:

$$i_{in}(n) = \frac{1}{N}\sum_{k=0}^{N-1} I_{in}(k)\cdot e^{j\,2\pi kn/N} \qquad (7)$$

The computation complexity of relation (7) is $O(N^2)$. If the $N$ number of samples is not a prime number, it is possible to optimize the computation by properly grouping some operations depending on the factorization of $N$. In this case, a faster algorithm can be obtained, which also causes FFT to be equivalent to a fast DFT. The maximum reduction in time computation takes place when $N$ is a multiple of 2, i.e. $N=2^p$. In this case, the Cooley-Tukey algorithm can be applied. The complexity of this algorithm, also known in literature as FFT-2 or "radix-2FFT", is $O(N\cdot log_2 N)$, [20], [21], [22].

### 3.1 The FFT algorithm

The FFT algorithm is optimized to perform the DFT (Discrete Fourier Transform) in less time. The DFT in its turn represents the application of the Fourier transform on the discrete form. Generally speaking, the Fourier transform applied to a continuous function $f(t)$ on the time domain supplies as a result a continuous function $F(f)$ on the frequency domain as shown in this relation:

$$F(f) = \int_{-\infty}^{+\infty} f(t)\cdot e^{-j2\pi ft}\cdot dt \qquad (8)$$

The inverse of the Fourier transform, which allows to pass from the frequency domain to the time domain, is shown in the following relation:

$$f(t) = \int_{-\infty}^{+\infty} F(f)\cdot e^{j2\pi ft}\cdot df \qquad (9)$$

It is useful to remember that functions $f(t)$ and $F(f)$ are continuous functions in the time and frequency domains, respectively.

Let us suppose to operate in the time domain on a discrete function, which means an $x(n)$ function consisting of a sequence of $N$ ($n=1, 2...., N$) samples, usually defined as $x(1), x(2), \ldots, x(N)$, as when $N$ measurement samples are acquired.

The examined $x(n)$ discrete function is a mono-dimensional array (vector) having dimension equal to $N$. The Fourier transform theory can also be applied to the $x(n)$ discrete function; in this case the algorithm is named Discrete Fourier Transform (DFT), and is reported in the following relation:

$$X(k) = \sum_{n=0}^{N-1} x(n)\cdot e^{-j\cdot 2\pi\frac{k}{N}\cdot n} \qquad k = 0,...,N-1 \qquad (10)$$

Relation (10) allows to pass from the $x(n)$ time domain to the $X(k)$ frequency domain. For the inverse operation, that is to say, passing from the $k\Delta f$ frequency domain to the $n\Delta t$ time domain, the Inverse Discrete Fourier Transform (IDFT) must be used, as reported below:

$$x(n) = \frac{1}{N}\cdot\sum_{k=0}^{N-1} X(k)\cdot e^{j\cdot 2\pi\frac{k}{N}\cdot n} \qquad n = 0,...,N-1 \qquad (11)$$

It must be always kept in mind that, similarly as for relations (4) and (5), also in relations (10) and (11) the sample intervals (both in the time domain ($\Delta t$) and frequency domain ($\Delta f$)) can be assumed as unitary values. In this case, formulas (10) and (11) are in their extended forms as follows:

$$X(k\Delta f) = \Delta t\sum_{n=0}^{N-1} x(n\Delta t)\cdot e^{-j\cdot 2\pi\cdot k\Delta f\cdot n\Delta t}$$

$$x(n\Delta t) = \Delta f\sum_{k=0}^{N-1} X(k\Delta f)\cdot e^{j\cdot 2\pi\cdot k\Delta f\cdot n\Delta t}$$

with $\Delta f = \frac{1}{N\cdot\Delta t}$.

The $X(k)$ components are imaginary numbers, which actually represent the modules and phases of the sinusoidal components of the $x(n)$ samples. The DFT allows to pass from $x(n)$ to $X(k)$, whereas the IDFT shows the $x(n)$ relation as a sum of sinusoidal components $\frac{X(k)}{N}e^{j\cdot 2\pi\frac{k}{N}\cdot n}$, with $\frac{k}{N}$ frequency per sample cycle.

The above explanation concerns the DFT applied to a vector of $N$ measured samples such as ($x(1), x(2),\ldots,x(N)$). In this case the DFT is also defined as mono-dimensional. In practical cases, the Fourier transform may sometimes need to be applied to a number of vectors obtained from different $(x_{n1}, x_{n2},\ldots,x_{nd})$ time intervals. In such cases the DFT is defined as multi-dimensional, but is mentioned only for completeness and was not used in the examined cases.

In order to compute the $X(k)$ through relation (10) directly, a number of arithmetical operations equal to $O(N^2)$ are required. In this case some operations linked to relation (10) can be grouped in order to obtain a less complex, faster algorithm. If the Fourier Transform is applied to a discrete signal composed of $N$ samples, a factorization of $N$ can be made, that is some operations will be adequately grouped so as to reduce computation time

considerably and obtain a "fast" algorithm of the DFT. The most widely used algorithm of this kind is the Cooley-Tukey algorithm, which is based on the *"divide et impera"* principle, that is to say a DFT is cut recursively off any *N* dimension where *N* is a number $N=N_1 \cdot N_2$ of smaller DFT having dimensions $N_1$ and $N_2$, respectively.

Let us suppose to have *N* samples *(x(1), x(2), …, x(N))* obtained from a measurement process and to perform the DFT on this vector. If the standard DFT algorithm is applied in order to compute all the *N* samples (*X(k)*, with *k=1,2, …, N* ), the number of complex multiplications to be performed is equal to $N^2$. In case the periodicity of the exponential function $e^{j\cdot 2\pi f\cdot t}=\cos(2\pi f\cdot t)+j\cdot\sin(2\pi f\cdot t)$ is exploited, it is possible to use the same complex multiplications many times, which allows the above mentioned factorization of the number of multiplications.

In order to perform the FFT algorithm, the first operation is to separate the *X(k)* former *N/2* frequency samples from the latter *N/2* samples with *k=1, 2, …, N*, where each *X(k)* term is obtained from the summation of relation (10). The second operation is a subdivision inside relation (10) of the terms with even indexes from those with odd indexes as shown in the following relation.

$$X(k)=\sum_{n=0}^{N-1}x(n)\cdot e^{j\cdot 2\pi\frac{k}{N}n}=\sum_{n=0}^{N-1}x(n)\cdot W^{n\cdot k}= \\ =\sum_{n=0}^{\frac{N}{2}-1}x(2n)\cdot W^{(2n)k}+\sum_{n=0}^{\frac{N}{2}-1}x(2n+1)\cdot W^{(2n+1)k} \quad (12)$$

with $k=0,1,...,\frac{N}{2}-1$.

From relation (12) the position $W=e^{j\cdot 2\pi\frac{1}{N}}$ can be assumed. In this case relation (12) becomes:

$$X(k)=X_1(k)+W^K\cdot\sum_{n=0}^{\frac{N}{2}-1}x(2n+1)\cdot W^{2nk}= \\ =X_1(k)+W^k\cdot X_2(k) \quad (13)$$

with $k=0,1,...,\frac{N}{2}-1$.

With relations (12) and (13) only the *N/2* frequency samples are considered (*X(k) (k=0, 1, …, N/2*) and inside their relation (*2k*) even terms were separated from the (*2k+1*) odd terms. The subsequent *N/2* samples of *X(k)* can be expressed through the following relation:

$$X\left(k+\frac{N}{2}\right)=X_1\left(k+\frac{N}{2}\right)+W^{k+\frac{N}{2}}\cdot X_2\left(k+\frac{N}{2}\right) \quad (14)$$

with $k=0,1,...,\frac{N}{2}-1$.

As previously mentioned, in order to reduce the number of multiplications of the DFT algorithm, the periodicity of the exponential function $e^{j\varphi}=\cos(\varphi)+j\cdot\sin(\varphi)$ is exploited obtaining the FFT. Actually, the complex multiplications used for the computation of the former *N/2* samples *X(k)* with (*k=0, 1, …, N/2*) can be reused also on the computation of the latter *N/2* samples *X(k)* (k=*N/2, N/2+1, …, N-1)* by using proper linkages between terms with even and odd indexes, respectively. The "decimation" relations at the basis for the procedure are the following:

$$X_1\left(k+\frac{N}{2}\right)=X_1(k) \quad (15)$$

$$W^{k+\frac{N}{2}}\cdot X_2\left(k+\frac{N}{2}\right)=-W^k\cdot X_2(k) \quad (16)$$

where $k=0,1,...,\frac{N}{2}-1$.

The equality of relation (16) can be understood with the following relation:

$$W^{(k+\frac{N}{2})}=e^{j\cdot 2\pi\frac{1}{N}(k+\frac{N}{2})}=e^{j\cdot 2\pi\frac{1}{N}\cdot kn}\cdot e^{j\cdot 2\pi\cdot\frac{1}{N}\cdot\frac{N}{2}}= \\ =e^{j\cdot 2\pi\frac{1}{N}\cdot k}\cdot e^{j\cdot 2\pi\cdot\frac{1}{N}\cdot\frac{N}{2}}=e^{j\cdot 2\pi\frac{1}{N}\cdot k}\cdot e^{j\cdot\pi}=-W^k \quad (17)$$

Finally, the *N* samples *X(k) (k=0, 1, …, N* of the *N* measures *(n) (n=0, 1, …, N)* can be obtained through the application of the FFT algorithm implemented with relations:

$$X(k)=X_1(k)+W^k\cdot X_2(k) \quad (18)$$

$$X\left(k+\frac{N}{2}\right)=X_1(k)-W^k\cdot X_2(k) \quad (19)$$

where $k=0,1,...,\frac{N}{2}-1$.

Relations (18) and (19) show that the former *N/2* samples X(k) (k=0, 1, …, $\frac{N}{2}-1$) change only the sign of the algebraic sum between the terms $X_1(k)$ and $W^k\cdot X_2(k)$; this allows to obtain also

the latter terms of the succession *X(k)* (with $k = \frac{N}{2}, \frac{N}{2}+1, ..., N-1$).

Fig. 11 shows the operation reduction by applying the Cooley-Tukey algorithm.

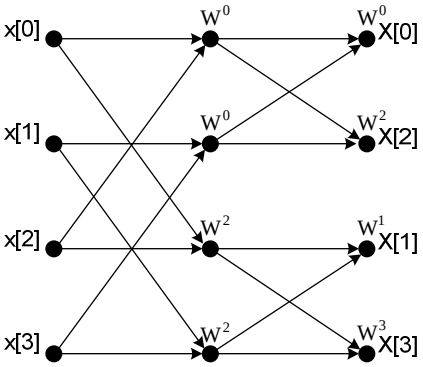


Fig. 11 Decimation process of the Cooley-Tukey algorithm.

When *N* samples are available, it is possible to operate a series of subsequent halved cuts to compute the *N* sample *X(k)*. If *N* is a power of 2: $N=2^p$ with $p \geq 1$. it is possible to have a number of halved cuts equal to $log_2(N)$. For each cut the number of complex multiplications are *N*. Finally, for a number of $N=2^p$ samples, the number of operations necessary to apply the FFT algorithm is $O(N \cdot \log_2(N))$ while the multiplications necessary for the DFT algorithm are $O(N^2)$.

## 4 Experimental and computation results

Fig. 12 shows the wave shape of the output current coming from the six-phase AC/DC converter when a resistive load of $R_{LOAD}$=0.03 Ω is applied.

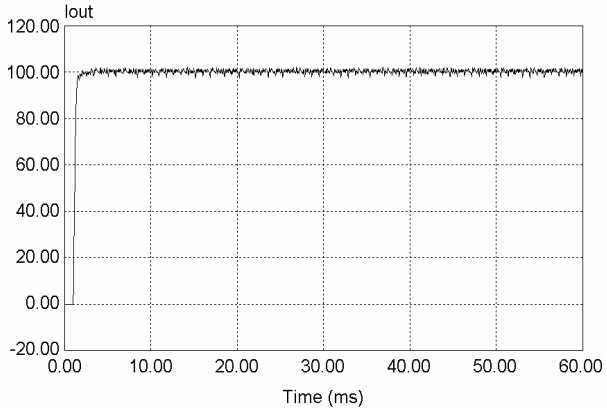


Fig. 12. Wave shape of the current present downstream of the six-phase AC/DC converter (output current = 100A).

In this situation, the reference current established for feed-back control was 100 A. Fig. 12 shows that the AC/DC output current follows the reference value imposed by the control system, if a very small ripple factor is neglected.

Figs. 13, 14 and 15 show the output current with an input reference of the control system ($I^*_{ref}$) of 200A, 300A and 400A respectively, with a load of $R_{LOAD}$=0.03 Ω.

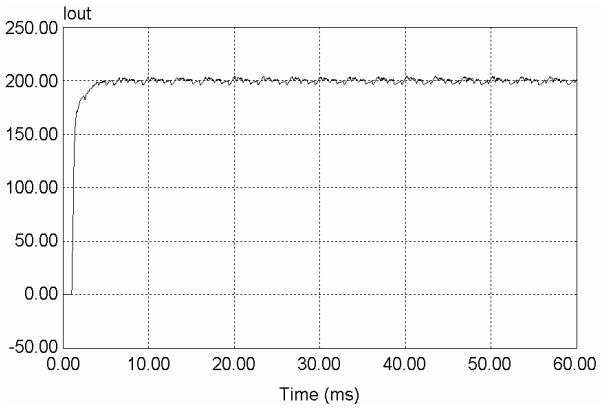


Fig. 13. Converter output current with an input current reference of 200 A.

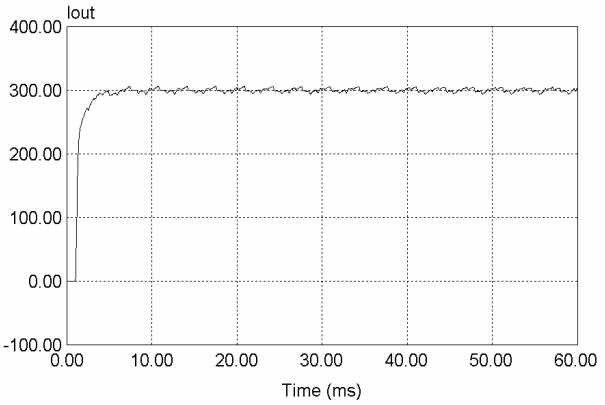


Fig. 14. Converter output current with an input current reference of 300 A.

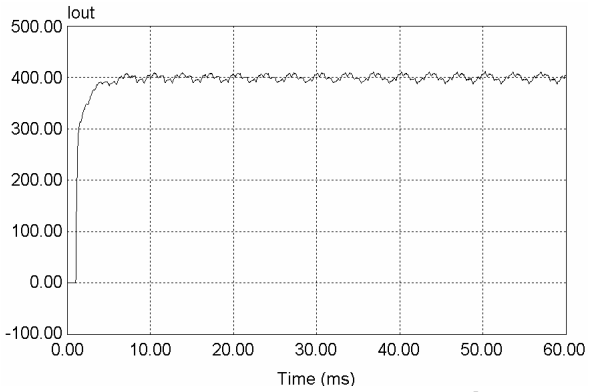


Fig. 15. Converter output current with an input current reference of 400 A.

The results obtained confirmed the correct behaviour of the proposed system.
The wave shape of the R-phase current upstream of the non-active three-phase rectifier is shown in Fig. 16. The value of the current peak is about 36A while the T period of the current wave is 20 ms, corresponding to a frequency of 50 Hz.

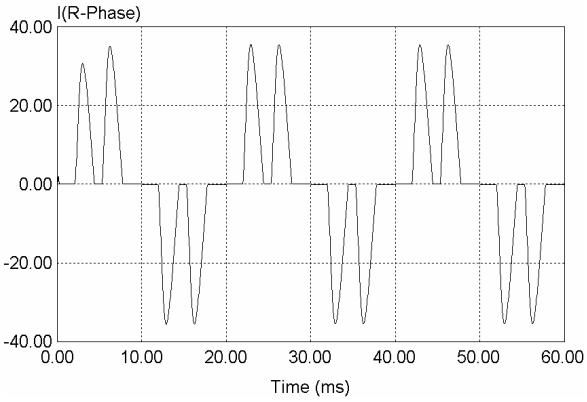


Fig. 16. Wave shape of the R-phase current drawn from the network.

The results of the FFT analysis applied to the phase current of Fig. 16 are shown in Fig. 17.

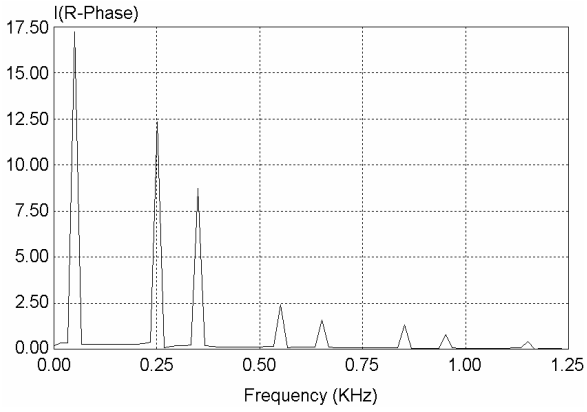


Fig. 15. Results of the FFT applied to the R-phase current drawn from the network.

The amplitude of the fundamental frequency and other harmonics are reported in table 1.
These results give rise to the following observations. The frequency of each subsequent harmonic is 100 - 200 Hz greater than the previous one, starting and proceeding alternatively from the fundamental frequency. As concerns amplitudes, the fundamental takes up a value of A/2, where A is the peak amplitude of the wave shape of the current drawn by the converter. The second harmonic takes up a value of A/2, the third harmonic A/3, the fourth harmonic A/4 and so on.

Table 1 Harmonic analysis of the current drawn from the supply network.

| Harmonic order | Frequency[Hz] | Amplitude[A] |
|---|---|---|
| 1 | 50,000 | 17,2295 |
| 2 | 250,000 | 11,8556 |
| 3 | 350,000 | 8,2671 |
| 4 | 550,000 | 2,2196 |
| 5 | 650,000 | 1,4334 |
| 6 | 850,000 | 1,2213 |
| 7 | 950,000 | 0,7399 |

Finally, table 2 shows the efficiency of the proposed converter.

Table 2 Efficiencies of the four-stage converter for different values of the output currents.

| Iout[A] | Pin[W] | Pout[W] | η |
|---|---|---|---|
| 100 | | 321 | 0,7 |
| 200 | 1714,28 | 1200 | 0,7 |
| 300 | 3802 | 2700 | 0,71 |
| 400 | 6857 | 5200 | 0,7 |
| 150 | 938,5 | 657 | 0,7 |
| 250 | 2678,57 | 1875 | 0,7 |
| 350 | 5250 | 3675 | 0,7 |

# 5 Conclusions

A new type of an AC/DC high current converter composed of four stages was presented. The first stage performed an AC/DC conversion while the second and fourth stages employed a specific switching procedure performing a DC/AC and AC/DC conversions, respectively. The fourth stage was supplied by an electric transformation section which was actually the third stage. The inverter commuted with a 40 kHz carrier frequency, and a 6-phase star rectifier was connected downstream the transformer. Experimental laboratory tests on a converter prototype validated the correct behaviour of the new architecture. Also a harmonic analysis of the current drawn from the supply network was performed using the FFT algorithm, and finally the shapes of the recorded output currents were reported and discussed. The proposed system could be effectively employed in fields requiring very high DC currents, such as electric traction and electrochemical applications.

*References:*

[1] S. Wu, L. B. Zhou, S.H. Huang, A study on doubly-fed induction machine with bi-directional AC/DC/AC converter, *Universities Power Engineering Conference, 2004 UPEC*

*2004 39th International*, Vol. 2, 6-8 Sept. 2004, pp. 575–581.

[2] Z. Wang, L. Chang, PWM AC/DC boost converter system for induction generator in variable-speedwind turbines, *Electrical and Computer Engineering, 2005 Canadian Conference on*, 1-4 May 2005, pp. 591–594.

[3] F. Muzi, C. Buccione, S. Mautone, A new architecture for systems supplying essential loads in the Italian High-Speed Railway (HSR), *WSEAS Transactions on Circuits and Systems*, Issue 8, Volume 5, August 2006.

[4] B. R. Lin, D. J. Chen, Single-phase neutral point clamped AC/DC converter with the function of power factor corrector and active filter, *Electric Power Applications, IEE Proceedings*, Vol. 149, Jan. 2002, pp. 19–30.

[5] F.C. Qun Zhao Lee, T. Fu Sheng, Voltage and current stress reduction in single-stage power factor correction AC/DC converters with bulk capacitor voltage feedback, *Power Electronics, IEEE Transactions on*, Vol. 17, July 2002, pp. 477–484.

[6] R. Morrison, M.G. Egan, A new modulation strategy for a buck-boost input AC/DC converter, *Power Electronics, IEEE Transactions on*, Vol. 16, Jan. 2001, pp. 34–45.

[7] L. Bor Ren, H. Chun Hao, Single-phase converter with flying capacitor topology, *TENCON 2004 2004 IEEE Region 10 Conference*, Vol. 4, 21-24 Nov. 2004, pp. 73–76.

[8] K. Y. Lee, H. Y. Hsu, Y. Lai, Simple Digital-Controlled AC/DC Converter with Power Factor Correction for Universal Input Applications, *Industrial Electronics Society, 2007* IECON 2007. 33rd Annual Conference of the IEEE, 5-8 Nov. 2007, pp. 1472–1477.

[9] E. Ngandui, P. Sicard, Probabilistic models of harmonic currents produced by twelve-pulseAC/DC converters, *Power Delivery, IEEE Transactions on*, Vol. 19, Oct. 2004, pp. 1898–1906.

[10] S. Saponara, P. Terreni, Cost-effective design of AC/DC converter with programmable powerAmplification, *Industrial Technology, 2004 IEEE ICIT '04 2004 IEEE International Conference on*, Vol. 1, 8-10 Dec. 2004, pp. 548–562.

[11] J. Mahdavi, S. Kaboli, H. A. Toliyat, Conducted electromagnetic emissions in unity power factor AC/DC converters: comparison between PWM and RPWM techniques, *Power Electronics Specialists Conference, 1999 PESC 99 30th Annual IEEE*, Vol. 2, 27 June-1 July 1999, pp. 881–885.

[12] A. N. Segura, P. B. Sanchez, Experimental measurement of non-characteristic harmonic power generated by thyristor pulse-controlled AC/DC three phase converters, *Industrial Electronics, 1996 ISIE '96, Proceedings of the IEEE International Symposium on*, Vol.1, 17-20 June 2006, pp. 549–554.

[14] P. Mattavelli, Design aspects of harmonic filters for high-power AC/DC converters, *Power Engineering Society Summer Meeting, 2000 IEEE*, Vol. 2, 16 – 20 July 2000, pp. 795-799.

[15] T. Matsukawa, M. Shioyama; Nomura, J.; Neumeyer, C.; Tsuji-Iio, S.; Shimada, R., Synchronous rectifier using power-MOSFET for high current AC/DC converter system, *Fusion Engineering, 2002 19th Symposium on*, 21-25 Jan. 2002, pp. 80–83.

[16] F. Muzi, A new digital power conditioner to improve quality and safety in electrical distribution systems, I*EEE-PES General Meeting*, June 6-10, 2004, Denver, Colorado, USA.

[17] S. D'Ottavi, F. Muzi, L. Passacantando, A real-time prediction procedure *of the state of an electrical distribution system, 6th WSEAS International Conference on Applications of Electrical Engineering*, Istanbul, Turkey, May 27-29, 2007.

[18] F. Muzi, L. Passacantando, A real-time monitoring and diagnostic procedure for electrical distribution networks**,** *International Journal of Energy*, (a NAUN, North Atlantic University Union, Journal), Issue 2, Vol. 1, 2007

[19] I. D. Lu, P. Lee, Use of mixed radix FFT in electric power system studies, *Power Delivery, IEEE Transactions on*, Vol. 9, July 1994, pp. 1297-1280.

[20]H. Sorensen, D. Jones, C. Burrus, Real-valued algorithms for the FFT, *Acoustics, Speech, and Signal Processing, IEEE International Conference on ICASSP '87*, Vol. 12, Apr.1987, pp. 1831-1834.

[21] D. Sundararajan, M. O. Ahmad, Swamy, M.N.S., Vector computation of the discrete Fourier transform, *Circuits and Systems II: Analog and Digital Signal Processing, IEEE Transactions on [see also Circuits and Systems II: Express Briefs, IEEE Transactions on]*, Vol. 45, April 1998, pp. 449-461.

[22] M. Puschel, Cooley-Tukey FFT like algorithms for the DCT, *Acoustics, Speech,*

*and Signal Processing, 2003. Proceedings. (ICASSP '03). 2003 IEEE International Conference on*, Vol. 2, 6-10 April 2003, pp. 501-504.

[23] C. Bartoletti, G. Fazio, F. Muzi, S. Ricci, G. Sacerdoti, Diagnostics of Electric Power Components: an improvement on signal discrimination, *WSEAS Transactions on circuits and systems*, Issue 7, Volume 4, July 2005.

[24] F. Muzi, An alternative FMECA procedure to design distribution system reliability, *WSEAS Transactions on Power Systems*, Issue 11, Volume 1, November 2006.

[25] F. Muzi, C. Buccione, S. Mautone, A new architecture for systems supplying essential loads in the Italian High-Speed Railway (HSR*), WSEAS Transactions on Circuits and Systems*, Issue 8, Volume 5, August 2006.